Optimized Model Predictive Control With Dead-Time Voltage Vector for PMSM Drives

Xiaoguang Zhang, *Member, IEEE*, Yu Cheng, Zhihao Zhao, and Kang Yan

***Abstract*—In order to improve the current steady-state control performance of the model predictive control (MPC), a dead-time voltage-vector based MPC method is proposed in this article. First, the effect of the dead-time on MPC is introduced, and the formation process of the dead-time voltage vector existed in MPC is analyzed. Furthermore, the beneficial dead-time voltage vector and nonbeneficial dead-time voltage vector for the current steady-state control performance of MPC is distinguished, and the advantage of the beneficial dead-time voltage vector is analyzed. Then, the MPC method based on dead-time voltage vector is presented, which optimizes the action time of dead-time. Finally, the experimental results prove that the current steady-state control performance of the proposed MPC method is better than the conventional MPC method without increasing the switching frequency.**

***Index Terms*—Dead time, model predictive control, PMSM.**

I. Introduction

PERMANENT magnet synchronous motor (PMSM) has many advantages, such as simple structure, small volume, high efficiency, and high power density [1]–[3]. With the industrial development, PMSM has been widely used in various occasions. In recent years, various control strategies have been introduced and applied in the PMSM control system. The most widely used method of PMSM control are field-oriented control (FOC) and the direct torque control. Meanwhile, other control methods also have been proposed and researched, such as sliding mode control [4], [5], fuzzy control [6], adaptive control [7], and model predictive control (MPC) [8], [9]. Among above-mentioned control methods, the MPC method received many attentions for its simple control structure and good dynamic performance [10]–[19].

Due to the different control object, MPC can be divided into two types of method, which are model predictive current control (MPCC) and model predictive torque control (MPTC) [20]–[22]. The MPTC method aims at the control of the stator flux linkage and electromagnetic torque. This means that the cost function of the MPTC needs weighting factor to balance the control of the stator flux linkage and electromagnetic torque. Unlike the MPTC method, the MPCC method takes motor current as the predictive variable and the cost function only consists of current error. Since motor currents have the same dimension, the cost function of the MPCC method does not need weighting factor, which means that the fussy weighting factor adjustment in the MPTC method can be avoided.

However, whatever control method is applied, a key problem, i.e., the existence of the dead-time, cannot be ignored. In various PMSM control systems, in order to protect the power supply from short circuit, the dead-time must be deployed to avoid short circuit between up and down IGBT of one bridge arm. It means that the dead-time will exist as long as the switching states change. Unfortunately, the existence of the dead-time will cause error of inverter output voltage and distortions of stator current. For the FOC method, there are some methods to overcome the influence of the dead-time effect. In the literature [23] and [24], the average theory based dead-time compensation method is presented, which uses the average voltage error to compensate the reference voltage. An $\delta\gamma$-axes is used instead of dq-axes to calculate the dead-time compensation voltage in [25]. A least-mean-square algorithm is introduced in [26], which focuses on eliminating the current harmonics caused by the dead-time effect. In [27], a simple disturbance estimator is proposed to compensate the voltage error caused by the dead-time effect.

However, due to the different applying mode of voltage vector, the dead-time effect of FOC and MPC methods is different. Therefore, dead-time compensation methods of FOC cannot be directly applied for the MPC. Few research works and solution about the dead-time effect of MPC method have been introduced so far [28]. The work in [29] proposes a compensation method of MPC, which considers the existence of dead-time and modifies the voltage vector included in the predictive model. In the literature [30], an MPC-based power control strategy for the grid-tie three-level neutral point clamped inverter is presented, and the dead-time effect is compensated by incorporating its influence in the prediction model. The work in [31] analyzes the reason that the dead-time increases the THD of the grid current and an algorithm correcting the negative impact of the dead-time by compensating the error voltage vector caused by the dead-time was proposed. An improved MPC-based common-mode voltage reduction method is proposed in [32] considering dead-time

Manuscript received February 1, 2020; revised June 10, 2020; accepted July 25, 2020. Date of publication July 30, 2020; date of current version October 30, 2020. This work was supported in part by the National Natural Science Foundation of China under Grant 51877002, in part by the Outstanding Young Scholars Fund of North China University of Technology, in part by the Young TopNotch Talents Program of Beijing Excellent Talents Funding (2017000026833ZK12), in part by the Fundamental Research Funds for Beijing Universities under Project 110052971921/025, in part by the Young TopNotch Talents Program for Municipal Universities of Beijing (CIT&TCD201904011), and in part by the 2019 Beijing Nova Program (Z191100001119036). Recommended for publication by Associate Editor T. Shi. *(Corresponding author: Xiaoguang Zhang.)*

The authors are with the North China University of Technology, Beijing 100144, China (e-mail: zhangxg123456789@163.com; 1434376387@qq.com; 625632961@qq.com; 729857315@qq.com).

Color versions of one or more of the figures in this article are available online at https://ieeexplore.ieee.org.

Digital Object Identifier 10.1109/TPEL.2020.3012985

effects, in which the effects of dead-time on the common-mode voltage are analyzed in detail. The abovementioned methods can achieve dead-time compensation of MPC, but the dead-time advantage without switching action is not fully exploited.

Existing MPC methods considering the dead-time can be regarded as a kind of passive compensation method, which mainly achieve steady-state performance increasing by compensating the voltage error caused by the dead-time. This passive compensation is not the optimal strategy to improve the system performance, since the dead-time advantage of MPC is not utilized. In this article, the dead-time process existed in the MPC is regarded as a dead-time voltage vector to increase the control freedom of MPC. Furthermore, the dead-time advantage without switching action is used reasonably. Therefore, the steady-state control performance of the conventional MPC method can be improved without increasing the average switching frequency.

The rest of this article is structured as follows. In Section II, the dead-time effect on the MPCC method is discussed in detail by the vector diagram and current simulation results. Next, Section III details the proposed MPC based on the dead-time voltage vector. In Section IV, a comparative investigation between the proposed MPC method and conventional method is performed by experiment. Finally, the conclusion is given in Section VI.

II. Mathematical Model and Conventional MPCC Method of the PMSM

The mathematical model of PMSM in the *d–q* rotating coordinate system is shown as follows:

$$\begin{cases} u_d = Ri_d + L \cdot di_d/dt - \omega_e L i_q \\ u_q = Ri_q + L \cdot di_q/dt + \omega_e L i_d + \omega_e \psi_f \end{cases} \tag{1}$$

where u_d and u_q are, respectively, the *dq*-axes voltages, i_d and i_q denote, respectively, the actual *dq*-axes currents, and ω_e represents the electrical rotor speed (rad/s). *R*, *L*, and ψf denote the winding resistance, stator inductance, and permanent magnet flux linkage, respectively. Besides, the surface-mounted permanent magnet synchronous motor (SPMSM) is applied in this article; thus, the *d*-axis inductance L_d is equal to the *q*-axis inductance L_q ($L = L_d = L_q$).

Then, based on (1), the current predictive model can be written as follows:

$$\begin{cases} i_d^p(k+1) = A \cdot i_d(k) + B \cdot i_q(k) + T/L \cdot u_d(k+1) \\ i_q^p(k+1) = A \cdot i_q(k) - B \cdot i_d(k) + T/L \cdot u_q(k+1) - C \end{cases} \tag{2}$$

where $A = 1 - TR/L$, $B = T\omega_e$, $C = T\omega_e\psi_f/L$, and *T* represents the control period.

According to the predictive model, the currents generated by the different voltage vector can be predicted. Then, the cost function (3) is used as the evaluation criterion. The voltage vector that minimizes the value of cost function is considered as the optimal voltage vector

$$g = \left[i_d^* - i_d(k+1)\right]^2 + \left[i_q^* - i_q(k+1)\right]^2. \tag{3}$$

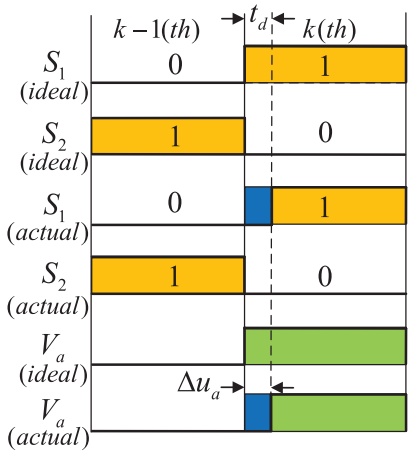

Fig. 1. PWM signal and output phase voltage.

III. Analysis of Dead-Time Effect and Principle in Conventional MPCC Method

A. Dead-Time Effect of Inverter Output Voltage

In practical application, the dead-time must be applied in PWM control period to avoid power supply short circuit. The ideal and actual PWM signals are shown in Fig. 1 under the condition of the dead-time (in Fig. 1, t_d is the action time of dead-time, which represents the time length of dead-time.)

From Fig. 1, it can be seen that the existence of dead-time causes distorted voltage error, which can be expressed by Δu_n as follows:

$$\Delta u_n = -\frac{t_d}{T} U_{\mathrm{dc}} \cdot \mathrm{sign}(i_x) \tag{4}$$

where i_x ($x = a, b, c$) represents the phase current, $\mathrm{sign}(i_x)$ denotes a sign function, and U_{dc} stands for the inverter dc-bus voltage. Furthermore, based on (4), the average three-phase voltage error can be expressed as follows:

$$\begin{cases} \Delta u_a = |\Delta u_n| \cdot \left[\frac{2\mathrm{sign}(i_a) - \mathrm{sign}(i_b) - \mathrm{sign}(i_c)}{3}\right] \\ \Delta u_b = |\Delta u_n| \cdot \left[\frac{2\mathrm{sign}(i_b) - \mathrm{sign}(i_a) - \mathrm{sign}(i_c)}{3}\right] \\ \Delta u_c = |\Delta u_n| \cdot \left[\frac{2\mathrm{sign}(i_c) - \mathrm{sign}(i_b) - \mathrm{sign}(i_a)}{3}\right]. \end{cases} \tag{5}$$

By Fourier series, the voltage error can be rewritten as follows [26]:

$$\begin{cases} \Delta u_a = \frac{4|\Delta u_n|}{\pi} \cdot \left[\sin(\omega t) + \sum_{n=6k\pm1}^{\infty} \frac{\sin(n\omega t)}{n}\right] \\ \Delta u_b = \frac{4|\Delta u_n|}{\pi} \cdot \left[\sin(\omega t - \frac{2}{3}\pi) + \sum_{n=6k\pm1}^{\infty} \frac{\sin(n\{\omega t - \frac{2}{3}\pi\})}{n}\right] \\ \Delta u_c = \frac{4|\Delta u_n|}{\pi} \cdot \left[\sin(\omega t + \frac{2}{3}\pi) + \sum_{n=6k\pm1}^{\infty} \frac{\sin(n\{\omega t + \frac{2}{3}\pi\})}{n}\right]. \end{cases} \tag{6}$$

The above analysis proves that the existence of the dead-time will cause the voltage error between ideal and actual output voltage. And this voltage error is mainly determined by the direction of current and the dead-time.

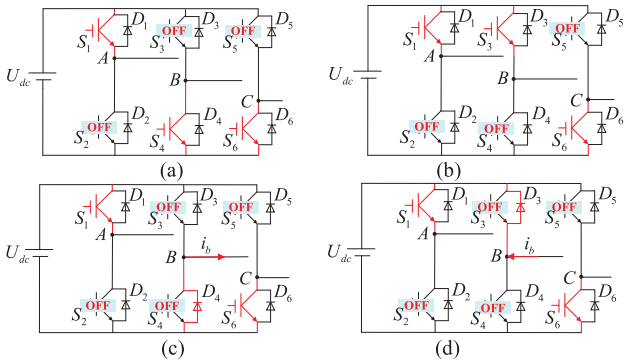

Fig. 2. Vector switching states. (a) Switching state of $U_1(100)$ at the ($k-1$)th control period. (b) switching state of $U_2(110)$ at the (k)th control period. (c) Dead-time voltage vector is$U_1(100)$under the condition of $i_b > 0$. (d) Dead-time voltage vector is $U_2(110)$ under the condition of $i_b < 0$.

B. Dead-Time Voltage Vector and Its Effect on MPC Method

For the conventional MPC method, only one optimal voltage vector is applied, i.e., switching states only update at the beginning of each control period. Thus, the dead-time is only deployed at the beginning of each control period. However, it is noteworthy that not every bridge arm needs to deploy the dead-time in each control period. Specifically, if the switching states of a bridge arm at the (k)th control period is different from that at the ($k-1$)th control period, the dead-time should be applied in control period. But if the switching states of a bridge arm at the (k)th control period is same as that at the (k-1)th control period, dead-time does not need to be inserted.

Taking the vector $U_1(100)$ and $U_2(110)$ as an example to analyze the influence of dead-time on MPC. Suppose that vector $U_1(100)$ is selected as the optimal voltage vector at the ($k-1$)th control period and $U_2(110)$ is selected as the optimal vector at the (k)th control period. The switching states of vector $U_1(100)$ and $U_2(110)$ are shown in Fig. 2(a) and (b).

From Fig. 2(a) and (b), it can be seen that from the ($k-1$)th control period to the (k)th control period, phases *A* and *C* do not change switching states. This means that phases *A* and *C* do not need to insert dead-time. Therefore, phases *A* and *C* both maintain these switching states between the ($k-1$)th control period and the (k)th control period. However, phase *B* needs to insert dead-time, since the switching state changes between the ($k-1$)th control period and the (k)th control period. Thus, two switches (S_3 and S_4) of phase *B* need to be turned OFF during dead-time t_d, as shown in Fig. 2(c) and (d). It should be noted that the state of phase *B* during dead-time t_d is determined by the sign of phase current. As shown in Fig. 2(c), when current direction of phase *B* is positive, the diode D_4 will conduct, which means that the switching state is the same as vector $U_1(100)$ under the condition of existence of phase *B* dead-time. In this article, the voltage vector generated by dead-time is called as dead-time voltage vector (U_{deadtime}). Thus, the dead-time voltage vector (U_{deadtime}) is $U_1(100)$, when the current direction of phase *B* is positive. On the other hand, when the current direction of phase *B* is negative, the diode D_3 will conduct and the dead-time voltage vector is $U_2(110)$, as shown in Fig. 2(d). Similarly, when

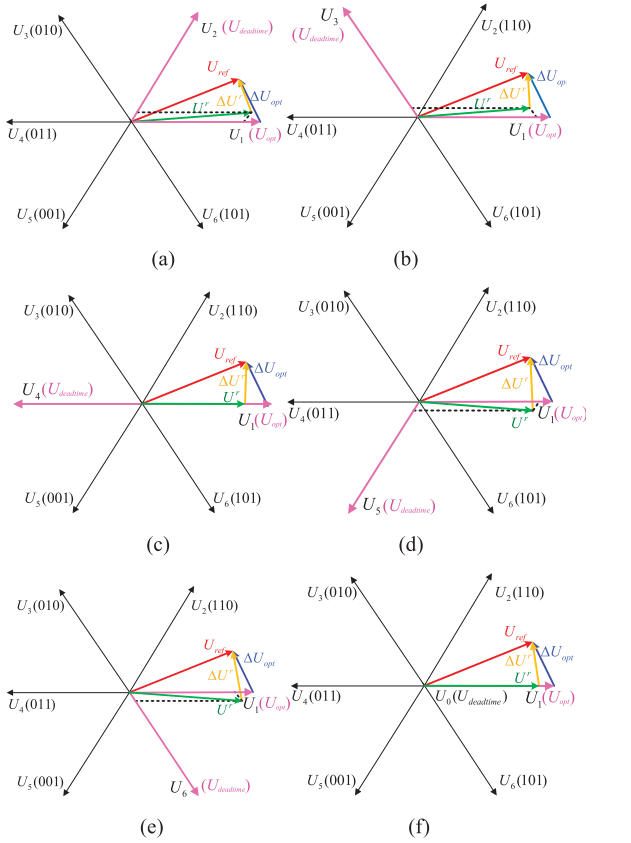

Fig. 3. Diagram of the selected voltage vector ($U_1(100)$) and dead-time voltage vectors. (a) Dead-time voltage vector is $U_2(110)$. (b) Dead-time voltage vector is $U_3(010)$. (c) Dead-time voltage vector is $U_4(011)$. (d) Dead-time voltage vector is $U_5(001)$. (e) Dead-time voltage vector is $U_6(101)$. (f) Dead-time voltage vector is $U_0(000)$.

different phases exist dead-time, different dead-time voltage vectors can be generated during the dead-time. Therefore, it can be seen that the dead-time voltage vector is determined by the current direction of phase that needs to insert the dead-time.

In order to facilitate the analysis of the influence of the dead-time voltage vector (U_{deadtime}) on the control performance of MPC, the dead-time is supposed to exist all the time and the voltage vector $U_1(100)$ is assumed to be the selected optimal voltage vector (U_{opt}). Fig. 3 shows the voltage error between the reference voltage vector and the actual selected voltage vector, when different dead-time voltage vector exists.

As shown in Fig. 3(a), when the dead-time voltage vector is $U_2(110)$, the actual applied voltage vector (U^r) consists of selected vector $U_1(100)$ and dead-time vector $U_2(110)$. In Fig. 3, ΔU_{opt} represents the voltage vector error between the reference voltage vector (U_{ref}) and ideal voltage vector, and ΔU^r denotes the voltage vector error between the reference voltage vector (U_{ref}) and actual applied voltage vector. It is obviously from Fig. 3(a) that ΔU^r is smaller than ΔU_{opt} when the dead-time voltage vector is $U_2(110)$. This means that the existence of dead-time voltage vector $U_2(110)$ improves the control performance of MPC.

Similarly, when the dead-time voltage vector is $U_3(010)$, $U_4(011)$, and $U_0(000)$, the voltage vector error is shown in

TABLE I
ERROR COMPARISON OF DIFFERENT DEAD-TIME VOLTAGE VECTOR WHEN THE SELECTED VOLTAGE VECTOR IS $U_1(100)$

Selected voltage vector	Dead-time voltage vector	Error comparison
$U_1(100)$	$U_1(100)$	$\Delta U^r = \Delta U_{opt}$
	$U_2(110)$	$\Delta U^r < \Delta U_{opt}$
	$U_3(010)$	$\Delta U^r < \Delta U_{opt}$
	$U_4(011)$	$\Delta U^r < \Delta U_{opt}$
	$U_5(001)$	$\Delta U^r > \Delta U_{opt}$
	$U_6(101)$	$\Delta U^r > \Delta U_{opt}$
	$U_0(000)/U_7(111)$	$\Delta U^r < \Delta U_{opt}$

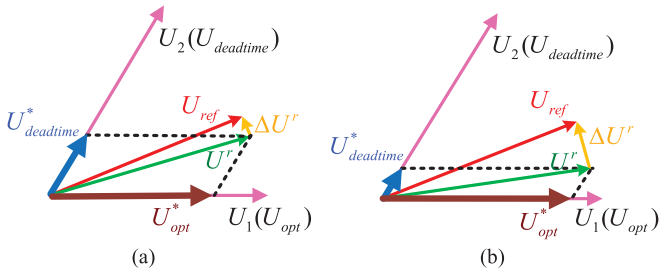

Fig. 4. Diagram of the selected voltage vector $(U_1(100))$ and dead-time voltage vector $(U_2(110))$ under different action times of dead-time vector. (a) Longer action time of a dead-time vector and (b) shorter action time of dead-time vector.

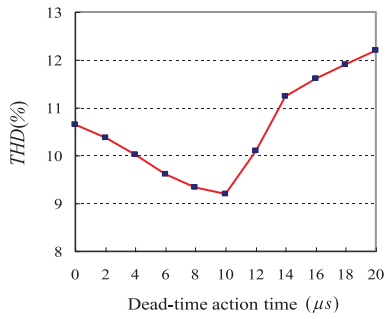

Fig. 5. THD analysis results of phase current under different dead-time action time.

TABLE II
PARAMETERS OF SIMULATION AND EXPERIMENT

Parameter	Description	Value
P	Number of pole pairs	2
L(mH)	Stator inductances	7.5
ψ_f (Wb)	Magnet flux linkage	0.325
$R(\Omega)$	Resistance	3.18
J(kg.m^2)	Rotational inertia	0.00046
T_{eL}(N.m)	Rated load torque	5
N(r/min)	Motor speed (Rated speed is 2000r/min)	1000
T(s)	Control period	0.0000666
V_{DC}(V)	DC Voltage	310

Fig. 3(b), (c), and (f), respectively. The same conclusion as Fig. 3(a) can be obtained, i.e., the existence of dead-time voltage vectors $U_3(010)$, $U_4(011)$, and $U_0(000)$ can also improve the control performance of MPC.

However, the conclusion is different, the dead-time voltage vector is $U_5(001)$ and $U_6(101)$, respectively, as shown in Fig. 3(d) and (e). It is obvious that ΔU^r is bigger than $\Delta U_{\rm opt}$, which means that the dead-time vectors $U_5(001)$ and $U_6(101)$ decrease the control performance of MPC.

When the selected voltage vector is $U_1(100)$, the voltage vector error comparison under different dead-time voltage vector situations is shown in Table I. It can be seen that four situations of dead-time voltage vectors $(U_2(110), U_3(010), U_4(011)$, and $U_0(000))$ can improve the control performance of the conventional MPCC method. Besides, two cases of dead-time voltage vectors $(U_5(001)$ and $U_6(101))$ will deteriorate the control performance of MPC.

According to the above analysis, most dead-time voltage vectors are beneficial to the control performance of the MPC system. However, it is well known that the action time of voltage vector has important influence on the control performance of the system. Thus, it is necessary to test the influence of the action time of these beneficial dead-time voltage vectors (i.e., the action time of dead-time) on the control performance of the MPC method. Assuming that the selected vector and dead-time vector are $U_1(100)$ and $U_2(100)$, respectively, Fig. 4 shows the vector diagram under different action times of the dead-time vector. $U^*_{\rm deadtime}$ and $U^*_{\rm opt}$ represent the actual dead-time voltage vector and optimal voltage vector, which are applied on motor. In can be seen that the voltage vector error (ΔU^r) between the reference voltage vector $(U_{\rm ref})$ and synthetic voltage vector (U^r) in Fig. 4(a) is smaller than that in Fig. 4(b). It means that the action time of the dead-time vector (i.e., the action time of a dead-time) is also an important factor to influence the control performance of MPC.

In order to test the specific impact of action time, the simulations are carried out under different dead-time action times. The simulation results of the phase current THD are shown in Fig. 5. And the parameters of simulation are shown in Table II. The simulation results imply that phase current harmonic content decreases when the dead-time action time expands within 10 μs. However, when the dead-time action time exceeds10 μs, phase current harmonic content increases with the continue increase of the dead-time action time. This means that the dead-time action time also will affect the current THD of the MPC system.

IV. PROPOSED CONTROL METHOD

According to the analysis, it can be found that the proper dead-time voltage vector and proper action time have benefit to reduce the current harmonic content of the MPC system. Therefore, it is very necessary to develop a control method to reasonably utilize dead-time voltage vectors and their action time. In this section, an MPC method based on the dead-time voltage vector is proposed to reduce the current harmonic content of MPC without the increase of the switching frequency.

The control diagram of the proposed method is shown in Fig. 6. The speed outer loop is controlled by a PI controller, and the output of the speed controller is used as the input of

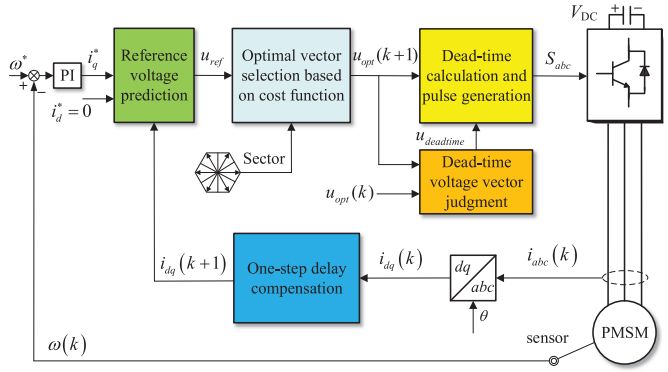

Fig. 6. Control diagram of the proposed method.

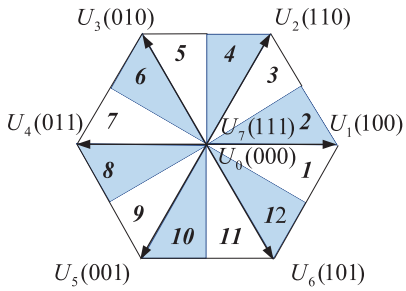

Fig. 7. Voltage vector sector.

reference voltage vector prediction. This predictive reference voltage is adopted as a judgment criterion to achieve fast optimal voltage-vector selection. Then, the dead-time voltage vector can be obtained based on the selected optimal voltage vector and the current direction, and its action time can be calculated. Finally, the switching pulses are generated to control the inverter. The following sections will introduce this method in detail.

A. Optimal Voltage Vector Selection

The sector-based fast vector selection method is adopted to avoid enumerating all eight candidate vectors at every control period [14]. Thus, the whole voltage vector plane is divided into 12 sectors, which is shown in Fig. 7. Every sector includes one nonzero voltage vector and one zero voltage vector (U_0 or U_7). Then, based on model (7)–(9), the reference voltage vector and its phase angle can be calculated as follows:

$$\begin{cases} u_d(k+1) = Ri_d(k) + L \cdot \frac{i_d^* - i_d(k)}{T} - \omega_e L i_q(k) \\ u_q(k+1) = Ri_q(k) + L \cdot \frac{i_q^* - i_q(k)}{T} + \omega_e L i_d(k) + \omega_e \psi_f \end{cases} \tag{7}$$

$$u_{ref} = \begin{pmatrix} u_\alpha \\ u_\beta \end{pmatrix} = \begin{pmatrix} \cos\theta & -\sin\theta \\ \sin\theta & \cos\theta \end{pmatrix} \begin{pmatrix} u_d(k+1) \\ u_q(k+1) \end{pmatrix} \tag{8}$$

$$\theta_{\text{ref}} = \arctan\left(\frac{u_\beta}{u_\alpha}\right). \tag{9}$$

Thus, the sector position of the reference voltage vector can easily be located by (9). Then, two candidate voltage vectors (one nonzero vector and one zero vector) included by the determined sector need to be evaluated by the cost function (3) to select the optimal voltage vector.

B. Dead-Time Voltage Vector Judgment

After the selection of optimal voltage vector of the next control period, the comparison between the selected optimal voltage vector and applied optimal voltage vector need to be achieved. If these two voltage vectors are the same vector, the dead-time does not need to be added. If these two voltage vectors are different vectors, the dead-time needs to be inserted. Then, the dead-time voltage vector is formed, and this dead-time voltage vector is determined by the current direction of the phase that needs to insert dead-time according to the analysis of Section III-B.

On the other hand, as mentioned above, not all dead-time voltage vectors are the beneficial vector for the MPC system. In addition, the action time of the dead-time voltage vector is also a key factor to influence the current steady-state control performance of MPC. Thus, it is necessary to distinguish these beneficial vectors when the reference voltage vector locates at different sectors. Then, the action time of these beneficial dead-time voltage vectors can be considered as a variable that needs to be optimized to reduce current harmonic content of MPC. However, the action time of dead-time voltage vectors that is not beneficial for the system control performance should be set as small as possible. In this article, in order to weaken the deterioration of control performance caused by a nonbeneficial dead-time voltage vector, the dead-time should be set as shorter as possible. According to the datasheet, the minimum dead-time of the inverter module used on hardware platform is 2 μs. In order to ensure experimental safety, the deployment of dead-time requires some margin. Therefore, the action time of nonbeneficial dead-time is set as 2.5 μs.

Table III lists the beneficial dead-time voltage vectors (the action time of dead-time can be adjusted on line) and nonbeneficial dead-time voltage vectors (the action time of the dead-time is fixed) at different sectors. In Table III, the dead-time voltage vectors whose action time can be treated as a variable are classified as group A. Besides, the group B contains dead-time voltage vectors whose action time is set as 2.5 μs. In real applications, after the selection of a optimal voltage vector, the dead-time voltage vector can be obtained. Then, according to Table III, whether this dead-time voltage vector is beneficial can be judged.

C. Action Time Calculation of Dead-Time

The determination principle of the dead-time duration can be divided into two categories. For the first category, after the selected optimal vector is determined, if the dead-time voltage vector is one of group *A*, the action time of this dead-time is regarded as a variable. According to voltage equation (1), the current slope of PMSM caused by the selected optimal voltage vector and dead-time voltage vector can be obtained as follows:

$$S_{\text{opt}} = \dot{i}_s = \frac{u_{\text{opt}} - Ri_s - e_s}{L} \tag{10}$$

$$S_{\text{deadtime}} = \dot{i}_s = \frac{u_{\text{deadtime}} - Ri_s - e_s}{L}. \tag{11}$$

TABLE III
DEAD-TIME VOLTAGE VECTOR GROUP AT DIFFERENT SECTOR.

Sector	Variable dead-time (group *A*)	Fixed dead-time (group *B*)
1	$U_4(011)$, $U_5(001)$, $U_6(101)$, $U_0(000)$, $U_7(000)$	$U_2(110)$, $U_3(010)$
2	$U_2(110)$, $U_3(010)$, $U_4(011)$, $U_0(000)$, $U_7(000)$	$U_5(001)$, $U_6(101)$
3	$U_1(100)$, $U_5(001)$, $U_6(101)$, $U_0(000)$, $U_7(000)$	$U_3(010)$, $U_4(011)$
4	$U_3(010)$, $U_4(011)$, $U_5(001)$, $U_0(000)$, $U_7(000)$	$U_1(100)$, $U_6(101)$
5	$U_1(100)$, $U_2(110)$, $U_6(101)$, $U_0(000)$, $U_7(000)$	$U_4(011)$, $U_5(001)$
6	$U_4(011)$, $U_5(001)$, $U_6(101)$, $U_0(000)$, $U_7(000)$	$U_1(100)$, $U_2(110)$
7	$U_1(100)$, $U_2(110)$, $U_3(010)$, $U_0(000)$, $U_7(000)$	$U_5(001)$, $U_6(101)$
8	$U_1(100)$, $U_5(001)$, $U_6(101)$, $U_0(000)$, $U_7(000)$	$U_2(110)$, $U_3(010)$
9	$U_2(110)$, $U_3(010)$, $U_4(011)$, $U_0(000)$, $U_7(000)$	$U_1(100)$, $U_6(101)$
10	$U_1(100)$, $U_2(110)$, $U_6(101)$, $U_0(000)$, $U_7(000)$	$U_3(010)$, $U_4(011)$
11	$U_3(010)$, $U_4(011)$, $U_5(001)$, $U_0(000)$, $U_7(000)$	$U_1(100)$, $U_2(110)$
12	$U_1(100)$, $U_2(110)$, $U_3(010)$, $U_0(000)$, $U_7(000)$	$U_4(011)$, $U_5(001)$

Therefore, the current at the end of the control period can be expressed as follows:

$$i_s(k+1) = i_s(k) + S_{\text{opt}} \cdot t_1 + S_{\text{deadtime}} \cdot (T - t_1). \quad (12)$$

Then, based on the principle of current deadbeat control (i.e., $i_s^* = i_s(k+1)$), the following expression can be obtained:

$$t_1 = \frac{[i_s^* - i_s(k) - S_{\text{opt}} \cdot T] \cdot (S_{\text{deadtime}} - S_{\text{opt}})}{(S_{\text{deadtime}} - S_{\text{opt}}) \cdot (S_{\text{deadtime}} - S_{\text{opt}})} \quad (13)$$

where t_1 is the action time of the selected optimal voltage vector; T-t_1 represents action time of dead-time; and i_s^* and $i_s(k)$ are the reference current and actual current, which can be expressed as $i_s^* = i_d^* + j \cdot i_q^*$ and $i_s(k) = i_d(k) + j \cdot i_q(k)$, respectively. Moreover, the current slope of S_{opt} and S_{deadtime} can be calculated as follows:

$$\begin{cases} S_{d\_\text{opt}} = \frac{u_{d\_\text{opt}} + [-Ri_d(k) + \omega_e L i_q(k)]}{L} \\ S_{q\_\text{opt}} = \frac{u_{q\_\text{opt}} + [-Ri_q(k) - \omega_e L i_q(k) - \omega_e \psi_f]}{L} \end{cases} \quad (14)$$

$$\begin{cases} S_{d\_\text{deadtime}} = \frac{u_{d\_\text{deadtime}} + [-Ri_d(k) + \omega_e L i_q(k)]}{L} \\ S_{q\_\text{deadtime}} = \frac{u_{q\_\text{deadtime}} + [-Ri_q(k) - \omega_e L i_q(k) - \omega_e \psi_f]}{L} \end{cases}. \quad (15)$$

Based on (13)–(15), the expression of t_1 can be rewritten as follows:

$$t_1 = \frac{(x_q + x_d)}{(S_{q\_\text{deadtime}} - S_{q\_\text{opt}})^2 + (S_{d\_\text{deadtime}} - S_{d\_\text{opt}})^2} \quad (16)$$

where

$$x_d = [i_d^* - i_d(k) - S_{d\_\text{opt}} \cdot T] \cdot (S_{d\_\text{deadtime}} - S_{d\_\text{opt}})$$

$$x_q = [i_q^* - i_q(k) - S_{q\_\text{opt}} \cdot T] \cdot (S_{q\_\text{deadtime}} - S_{q\_\text{opt}}).$$

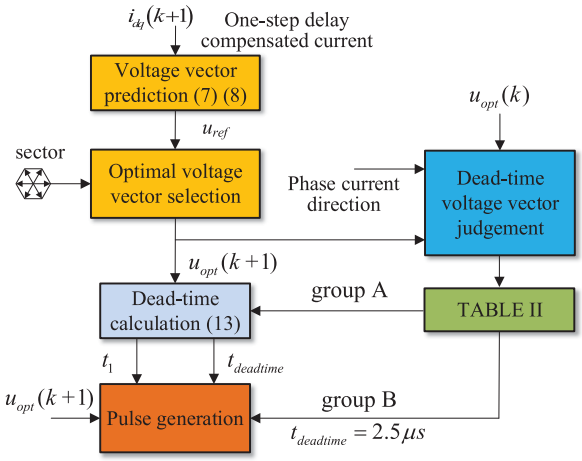

Fig. 8. Control flow diagram of the proposed method.

For the second category, after the selected optimal vector is determined, if the dead-time voltage vector belongs to group *B*, the action time of this dead-time is set as a fixed value (2.5 μs).

Furthermore, the flow diagram of the proposed method is shown in Fig. 8, and the control processes can be concluded as follows.

Step 1: $i_d(k+1)$and $i_q(k+1)$ can be obtained after one-step delay compensation based on the measured current.

Step 2: The optimal voltage vector can be quickly selected according to the reference voltage vector (7) and sector judgment result.

Step 3: Reference phase current (i_a^{ref}, i_b^{ref}, and i_c^{ref}) can be derived from *dq*-axes reference current (i_d^* and i_q^*) by coordinate transformation. Then, based on this reference phase current and the selected optimal vector, the dead-time voltage vector can be determined.

Step 4: The group of dead-time voltage vectors can be determined according to Table III.

Step 5: If the dead-time voltage vector belongs to group A, the action time of the dead-time is obtained by (13). Otherwise, the dead-time is set as 2.5 μs.

Step 6: The optimal voltage vector and dead-time is applied on the inverter.

Finally, it should be noted that although the dead-time voltage vector is adopted to reduce the current harmonic content, the switching frequency of the proposed MPC method is consistent with the conventional MPC method, because no switching action is needed when the dead-time is applied.

VI. EXPERIMENTAL RESULTS

In order to testify the effectiveness of the proposed method, the experiment is executed on the SPMSM hardware platform. The experimental parameters of the SPMSM control system is the same as the simulation parameters shown in Table II.

The current steady-state control performances of the conventional MPC method (with fixed dead-time) under the condition of different dead-time are shown in Fig. 9. From Fig. 9(a), it can

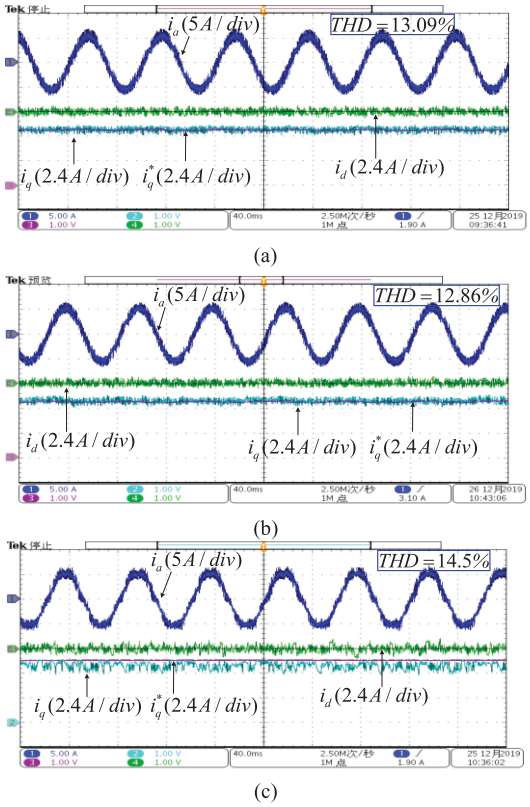

Fig. 9. Experimental results of the conventional MPC method under different dead-time conditions with rated load torque (5 N·m) at speed of 500 r/min. (a) Dead-time is set as2.5 μs. (b) Dead-time is set as5 μs. (c) Dead-time is set as14 μs.

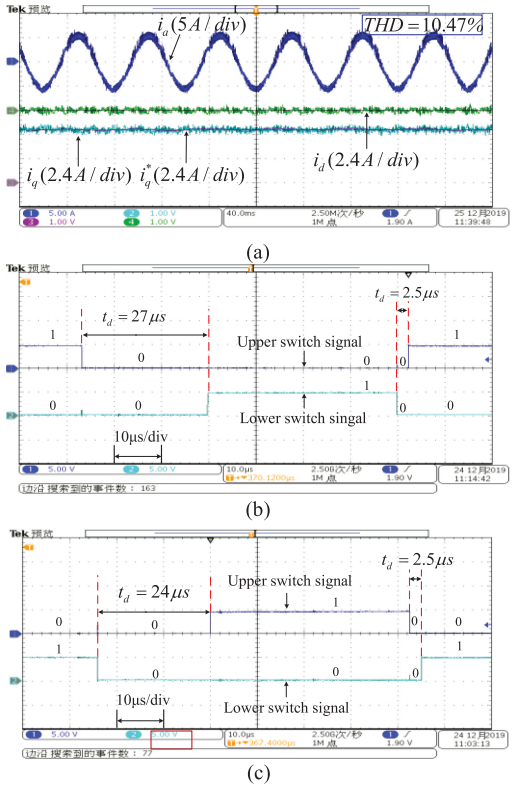

Fig. 10. Experimental results of the proposed MPC method with rated load torque (5 N·m) at speed of 500 r/min. (a) Current control performance. (b) Switching signals at one control instant. (c) Switching signals at another control instant.

be seen that the current THD is 13.09% when the dead-time is set as 2.5 μs; when the dead-time is increased to 5 μs, the current THD reduces form 13.09% to 12.86%, as shown in Fig. 9(b). This means that the extension of dead-time slightly reduces the current harmonic content of the MPC method. However, when the dead-time is further increased to 14 μs from 5 μs, the current THD increases from 12.86% to 14.5%. Moreover, the serious phase current distortion and *dq*-axes current oscillation can also be seen, as shown in Fig. 9(c). It means that overlong dead-time deteriorates the current steady-state control performance of conventional MPC. Above experimental results prove that the action time of dead-time will influence the current steady-state control performance of the MPC method; thus, it is necessary to optimize the dead-time duration.

In order to compare with the conventional MPC method shown in Fig. 9, the current waveforms of the proposed MPC method are given in Fig. 10(a). In addition, the pulse signals of two switching devices in phase *A* at different times is displayed in Fig. 10(b) and (c) under the control of the proposed method. Comparing Fig. 9 with Fig. 10(a), it can be seen that the current THD is reduced to 10.47%, which means that the current steady-state control performance of the proposed MPC method is obviously better than that of the conventional MPC method. And from Fig. 10(b) and (c), it is obvious that the action time of the dead-time will change at different control periods, when the proposed MPC method is applied.

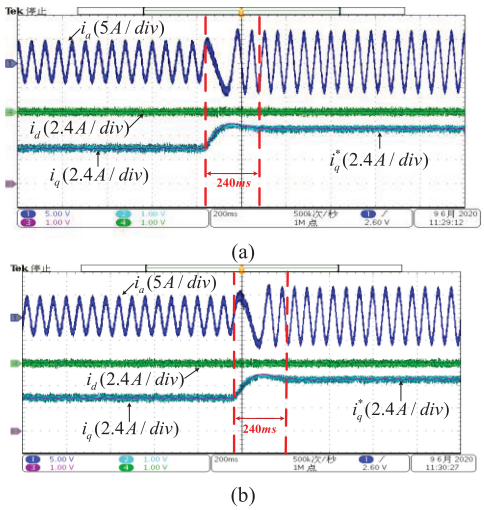

Fig. 11. Experimental results of two methods when load torque is suddenly increased from 3 to 5 N·m. (a) Conventional method (dead-time is set as 2.5 μs). (b) Proposed method.

Figs. 11 and 12 show the current waveform of two methods when load torque is suddenly changed. It can be seen that the dynamic response of the proposed method is similar to the conventional MPC method.

In addition, a comparison of upper switch number between the conventional MPC method and the proposed MPC method

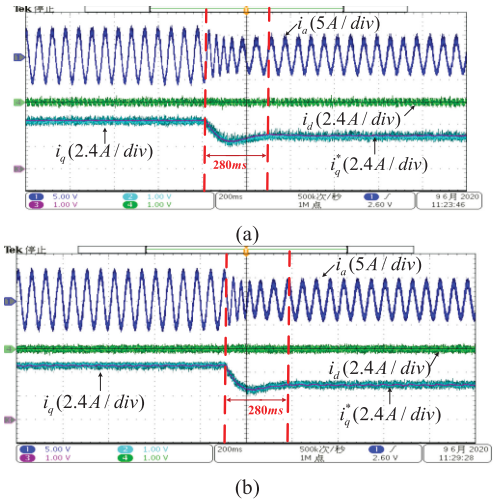

Fig. 12. Experimental results of two methods when load torque is suddenly decreased from 5 to 3 N·m. (a) Conventional method (dead-time is set as 2.5 μs). (b) Proposed method.

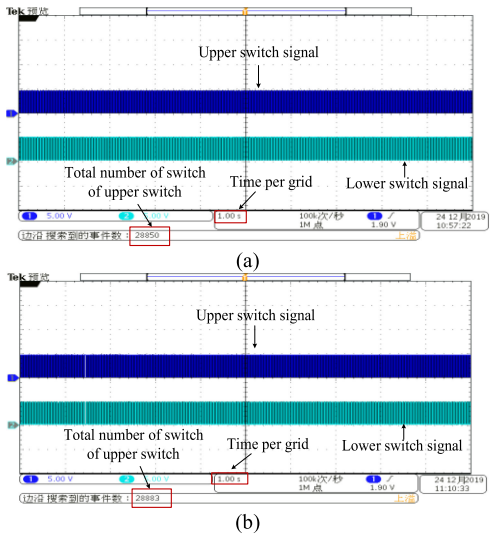

Fig. 13. Total number of switch of upper switch at the speed of 500 r/min with rated load torque. (a) Switch signal of conventional MPC method. (b) Switch signal of the proposed MPC method.

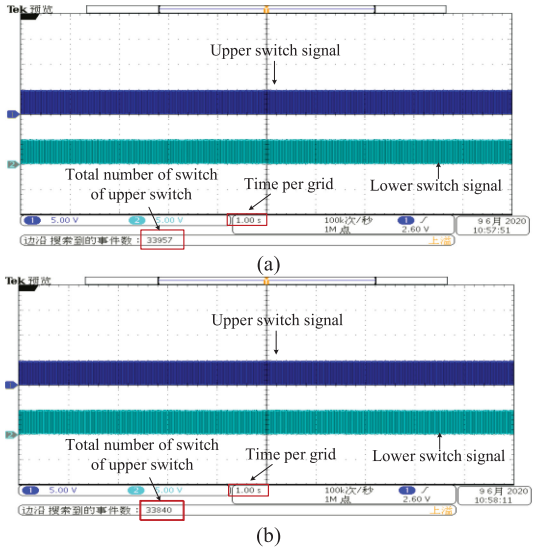

Fig. 14. Total number of switch of upper switch at the speed of 1000 r/min with rated load torque. (a) Switch signal of the conventional MPC method. (b) Switch signal of the proposed MPC method.

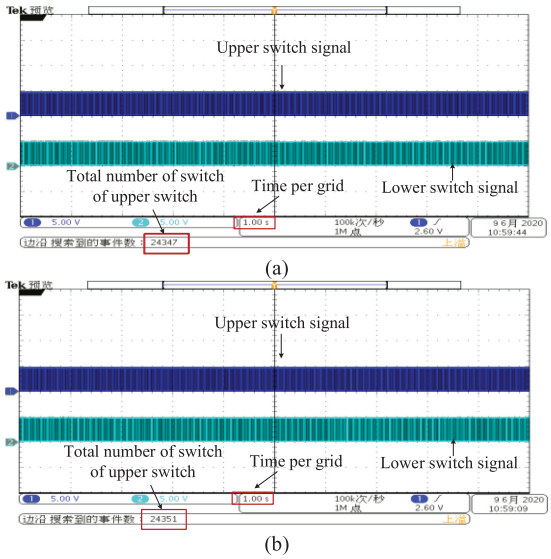

Fig. 15. Total number of switch of upper switch at the speed of 2000 r/min with rated load torque. (a) Switch signal of the conventional MPC method. (b) Switch signal of the proposed MPC method.

is shown in Fig. 13 under the same condition [at speed of 500 r/min and rated load torque (5 N·m)]. The total number of switches for the upper switch is 28 850 under the control of the conventional method; on the other hand, the total number of switches for the upper switch is 28 883 under the control of the proposed method. Therefore, the average switching frequency of two methods can be calculated by $f = N/t$, in which f represents the average switching frequency, N is the total number of switch and t represents the total time. This means that the average switching frequency f_1 of the conventional method is 2.885 kHz ($f_1 = 28850/10 = 2.88$ kHz), and the average switching frequency f_2 of the proposed method is 2.888 kHz ($f_1 = 28883/10 = 2.8883$ kHz). It can be seen that the average switching frequencies of both methods are similar, which indicates that the proposed method has better current steady-state control performance compared with the conventional method at the similar frequency.

Similarly, a switching frequency comparison under different conditions is shown in Fig. 14 (1000 r/min and rated load torque) and Fig. 15 (2000 r/min and rated load torque). When the motor speed is 1000 r/min, the average switching frequency of the conventional method and the proposed method is 3.395 kHz ($f_{1(1000\,r/\,\mathrm{min})} = 33\,957/10 = 3.395$ kHz) and 3.384 kHz ($f_{2(1000\,\mathrm{r/min})} = 33\,840/10 = 3.384$ kHz), respectively; when the motor speed is 2000 r/min, the average switching frequencies of two method are 2.434 kHz ($f_{1(2000\,r/\,\mathrm{min})} = 24\,347/10 = 2.434$ kHz) and 2.435 kHz ($f_{2(2000rpm)} = 24351/10 = 2.435$ kHz). This means that the

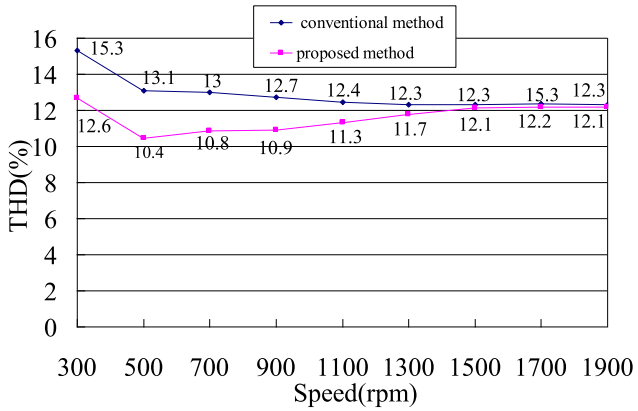

Fig. 16. Current THD comparison between the conventional method and the proposed method with rated load torque.

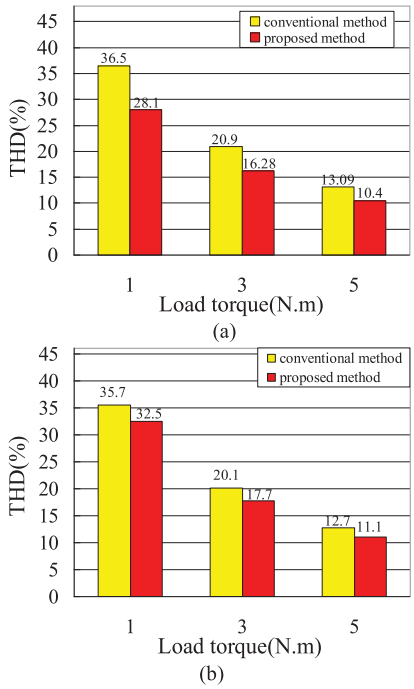

Fig. 17. Current THD comparison between the conventional method and the proposed method with different load torque, (a) at the speed of 500 r/min, (b) at the speed of 1000 r/min.

switching frequency of the proposed method is consistent with the conventional MPC method under different speed conditions.

The current THD performance comparisons between the conventional MPC method and the proposed MPC method under different speed conditions are shown in Fig. 16. It can be seen that the proposed MPC method has a lower current THD compared with the conventional MPC method at the whole speed operation range.

In addition, the current THD comparisons between the conventional MPC method and the proposed MPC method under the condition of different load torques are shown in Fig. 17. It can be seen that the proposed MPC method has a better performance compared with the conventional MPC method when different load torques are added at the same speed condition. In addition,

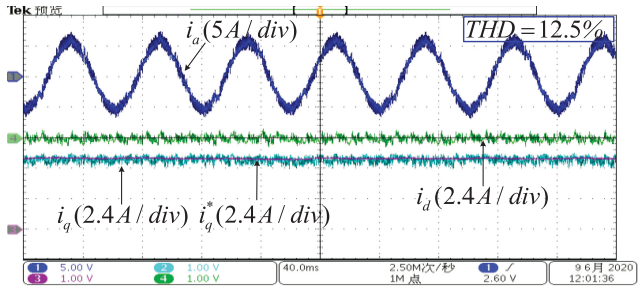

Fig. 18. Experimental result of the dead-time compensation proposed in [19].

the dead-time of the conventional MPC method in Figs. 16 and 17 is 2.5 μs.

In order to compare the current performance with other dead-time compensation methods, the experimental result of the dead-time compensation method proposed in [29] is shown in Fig. 18. And the experimental condition of Fig. 18 is consistent with Fig. 10. It can be seen that phase current harmonic content of Fig. 18 is higher than that of Fig. 10. Therefore, the current steady-state performance of the proposed method in this article is better than the dead-time compensation method proposed in [29].

In sum, experimental results verify that the proposed method can make full use of the dead-time effect to reduce the current harmonics and improve the current steady-state control performance of MPC without increasing the switching frequency.

VII. Conclusion

In this article, a model predictive control method based on the dead-time voltage vector is proposed. The main contributions are concluded as follows. 1) The dead-time voltage vector existed in MPC is analyzed and the beneficial vector and nonbeneficial vector are distinguished. 2) The novel MPC method that is able to optimize the action time of the dead-time is presented. Under the control of the proposed MPC method, the current harmonic content of the conventional MPC method is reduced without the increase of the switching frequency.

References

[1] Q. An, J. Liu, Z. Peng, L. Sun, and L. Sun, "Dual-Space vector control of open-end winding permanent magnet synchronous motor drive fed by dual inverter," *IEEE Trans. Power Electron.*, vol. 31, no. 12, pp. 8329–8342, Dec. 2016.

[2] X. Zhu, Z. Xiang, L. Quan, W. Wu, and Y. Du, "Multimode optimization design methodology for a flux-controllable stator permanent magnet memory motor considering driving cycles," *IEEE Trans. Ind. Electron.*, vol. 65, no. 7, pp. 5353–5366, Jul. 2018.

[3] G. Wang, J. Kuang, N. Zhao, G. Zhang, and D. Xu, "Rotor position estimation of PMSM in low-speed region and standstill using zero-voltage vector injection," *IEEE Trans. Power Electron.*, vol. 33, no. 9, pp. 7948–7958, Sep. 2018.

[4] X. Zhang, B. S. Hou, and Y. Mei, "Deadbeat predictive current control of permanent-magnet synchronous motors with stator current and disturbance observer," *IEEE Trans. Power Electron.*, vol. 32, no. 5, pp. 3818–3834, May 2017.

[5] X. Zhang and Z. Li, "Sliding-mode observer-based mechanical parameter estimation for permanent magnet synchronous motor," *IEEE Trans. Ind. Electron.*, vol. 31, no. 8, pp. 5732–5745, Aug. 2016.

[6] Y.-S. Kung, C.-C. Huang, and M.-H. Tsai, "FPGA realization of an adaptive fuzzy controller for PMLSM drive," *IEEE Trans. Ind. Electron.*, vol. 56, no. 8, pp. 2923–2932, Aug. 2009.
[7] H. Chaoui and P. Sicard, "Adaptive fuzzy logic control of permanent magnet synchronous machines with nonlinear friction," *IEEE Trans. Ind. Electron.*, vol. 59, no. 2, pp. 1123–1133, Feb. 2012.
[8] Z. Xiaoguang and H. Yikang, "Direct voltage-selection based model predictive direct speed control for PMSM drives without weighting factor," *IEEE Trans. Power Electron.*, vol. 34, no. 8, pp. 7838–7851, Aug. 2019.
[9] M. Liu, S. Wang, and M. Zou, "Improved robust deadbeat predictive current control for PMSM using stator current and disturbance observation," in *Proc. IEEE Int. Symp. Predictive Control Elect. Drives Power Electron.*, Quanzhou, China, 2019, pp. 1–5, doi: 10.1109/PRECEDE.2019.8753357.
[10] S. Vazquez *et al.*, "Model predictive control: A review of its applications in power electronics," *IEEE Ind. Electron. Mag.*, vol. 8, no. 1, pp. 16–31, Mar. 2014.
[11] Z. Xiaoguang, Z. Liang, and Z. Yongchang, "Model predictive current control for PMSM drives with parameter robustness improvement," *IEEE Trans. Power Electron.*, vol. 34, no. 2, pp. 1645–1657, Feb. 2019.
[12] X. Zhang, Y. Li, K. Wang, W. Zhang, and D. Gao, "Model predictive control of the open-winding PMSG system based on three-dimensional reference voltage-vector," *IEEE Trans. Ind. Electron.*, vol. 67, no. 8, pp. 6312–6322, Aug. 2020.
[13] B. Wang, X. Chen, Y. Yu, G. Wang, and D. Xu, "Robust predictive current control with online disturbance estimation for induction machine drives," *IEEE Trans. Power Electron.*, vol. 32, no. 6, pp. 4663–4674, Jun. 2017.
[14] X. Zhang and B. S. Hou, "Double vectors model predictive torque control without weighting factor based on voltage tracking error," *IEEE Trans. Power Electron.*, vol. 33, no. 3, pp. 2368–2380, Mar. 2018.
[15] X. Zhang, W. Zhang, C. Xu, Y. Li, Y. Wang, and D. Gao, "Three-dimensional vector based model predictive current control for open-end winding PMSG system with zero-sequence current suppression," *IEEE J. Emerg. Sel. Top. Power Electron.* to be published, doi: 10.1109/JESTPE.2019.2953805.
[16] Y. Luo and C. Liu, "A simplified model predictive control for a dual three-phase PMSM with reduced harmonic currents," *IEEE Tran. Ind Electron.*, vol. 65, no. 11, pp. 9079–9089, Mar. 2018.
[17] X. Zhang, Y. Cheng, Z. Zhao, and Y. He, "Robust model predictive direct speed control for SPMSM drives based on full parameter disturbances and load observer," *IEEE Trans. Power Electron.*, vol. 35, no. 8, pp. 8361–8373, Aug. 2020.
[18] X. Wei *et al.*, "Finite-control-set model predictive torque control with a deadbeat solution for pmsm drives," *IEEE Trans. Ind. Electron.*, vol. 62, no. 9, pp. 5402–5410, Sep. 2015.
[19] X. Zhang, Y. He, and B. Hou, "Double vector based model predictive torque control for SPMSM drives with improved steady-state performance," *J. Power Electron.*, vol. 18, no. 5, pp. 1398–1408, Sep. 2018.
[20] Y. Cho, K.-B. Lee, J.-H. Song, and Y. Lee, "Torque-ripple minimization and fast dynamic scheme for torque predictive control of permanent magnet synchronous motors," *IEEE Trans. Power Electron.*, vol. 30, no. 4, pp. 2182–2190, Apr. 2015.
[21] Y. Wang, X. Wang, and W. Xie, "Deadbeat model-predictive torque control with discrete space-vector modulation for PMSM drives of power converters and electrical drives," *IEEE Trans. Ind. Electron.*, vol. 64, no. 9, pp. 6930–6939, Sep. 2017.
[22] A. Mora and Á. Orellana, "Model predictive torque control for torque ripple compensation in variable-speed PMSMs," *IEEE Trans. Ind. Electron.*, vol. 63, no. 7, pp. 4584–4592, Jul. 2016.
[23] Y. Murai, T. Watanabe, and H. Iwasaki, "Waveform distortion and correction circuit for PWM inverters with switching lag-times," *IEEE Trans.Ind. Appl.*, vol. IA-23, no. 5, pp. 881–886, Sep./Oct. 1987.
[24] S.-G. Jeong and M.-H. Park, "The analysis and compensation of deadtime effects in PWM inverters," *IEEE Trans. Ind. Electron.*, vol. 38, no. 2, pp. 108–114, Apr. 1991.
[25] N. Urasaki and T. Senjyu, "An adaptive dead-time compensation strategy for voltage source inverter fed motor drives," *IEEE Trans. Power Electron.*, vol. 20, no. 5, pp. 1150–1160, Sep. 2005.
[26] Z. Tang and B. Akin, "A new LMS algorithm based deadtime compensation method for PMSM FOC drives," *IEEE Trans. Ind. Appl.*, vol. 54, no. 6, pp. 6472–6484, Jul. 2018.
[27] S.-Y. Kim and W. Lee, "Effective dead-time compensation using a simple vectorial disturbance estimator in PMSM drives," *IEEE Trans. Ind. Electron.*, vol. 57, no. 5, pp. 1609–1614, May 2010.
[28] M. Yang, K. Yang, G. Li, C. Yi, and D. Xu, "A novel dead-time compensation method for direct predictive control," in *Proc. 5th Int. Conf. Instrum. Meas. Comput. Commun. Control*, Qinhuangdao, 2015, pp. 273–277, doi: 10.1109/IMCCC.2015.64.
[29] A. Irnura, T. Takahashi, M. Fujitsuna, T. Zanma, and S. Doki, "Dead-time compensation in model predictive instantaneous-current control," in *Proc. IECON 2012 - 38th Annu. Conf. IEEE Ind. Electron. Soc.*, Montreal, QC, 2012, pp. 5037–5042, doi: 10.1109/IECON.2012.6388981.
[30] V.-Q.-B. Ngo, V.-H. Vu, and V.-T. Pham, "Lyapunov-induced model predictive power control for grid-tie three-level neutral-point-clamped inverter with dead-time compensation," *IEEE Access*, vol. 7, pp. 166869–166882, 2019.
[31] P. Falkowski and A. Sikorski, "Dead-time compensation in a new FCS-MPC of an AC/DC converter with a LCL filter," in *Proc. 13th Sel. Issu. Elect. Eng. Electron.*, Rzeszow, 2016, pp. 1–6, doi: 10.1109/WZEE.2016.7800201.
[32] L. Guo, N. Jin, C. Gan, L. Xu, and Q. Wang, "An improved model predictive control strategy to reduce common-mode voltage for two-level voltage source inverters considering dead-time effects," *IEEE Trans. Ind. Electron.*, vol. 66, no. 5, pp. 3561–3572, May 2019.

Xiaoguang Zhang (Member, IEEE) received the B.S. degree in electrical engineering from the Heilongjiang Institute of Technology, Harbin, China, in 2007, and the M.S. and Ph.D. degrees in electrical engineering from the Harbin Institute of Technology, Harbin, China, in 2009 and 2014, respectively.

He is currently a Distinguished Professor with the North China University of Technology, Beijing, China. From 2012 to 2013, he was a Research Associate with Wisconsin Electric Machines and Power Electronics Consortium, University of Wisconsin–Madison, Madison. He has published more than 50 technical papers in the area of motor drives. His current research interests include power electronics and electric machines drives.

Yu Cheng received the B.S. degree in electrical engineering in 2017 from the North China University of Technology, Beijing, China, where he is currently working toward the M.S. degree.

His current research interests include permanent magnet synchronous motor drives.

Zhihao Zhao was born in Henan, China, in 1996. He received the B.S. degree in electrical engineering in 2018 from the North China University of Technology, Beijing, China, where he is currently working toward the M.S. degree.

His current research interests include permanent magnet synchronous motor drives.

Kang Yan was born in Beijing, China, in 1997. He received the B.S. degree in electrical engineering in 2019 from the North China University of Technology, Beijing, China, where he is currently working toward the M.S. degree.

His current research interests include ac motor drives.